

University of Nebraska - Lincoln

DigitalCommons@University of Nebraska - Lincoln

Peter Dowben Publications

Research Papers in Physics and Astronomy

7-1-1994

Layer-by-layer growth of Hg on W(110)

Jiandi Zhang

University of Nebraska-Lincoln, jiandiz@lsu.edu

Dongqi Li

Syracuse University

Peter A. Dowben

University of Nebraska-Lincoln, pdowben@unl.edu

Follow this and additional works at: <https://digitalcommons.unl.edu/physicsdowben>



Part of the [Physics Commons](#)

Zhang, Jiandi; Li, Dongqi; and Dowben, Peter A., "Layer-by-layer growth of Hg on W(110)" (1994). *Peter Dowben Publications*. 120.

<https://digitalcommons.unl.edu/physicsdowben/120>

This Article is brought to you for free and open access by the Research Papers in Physics and Astronomy at DigitalCommons@University of Nebraska - Lincoln. It has been accepted for inclusion in Peter Dowben Publications by an authorized administrator of DigitalCommons@University of Nebraska - Lincoln.

Layer-by-layer growth of Hg on W(110)

Jiandi Zhang

Department of Physics, Syracuse University, Syracuse, New York 13244-1130 and Department of Physics, University of Nebraska-Lincoln, Lincoln, Nebraska 68588-0111

Dongqi Li

Department of Physics, Syracuse University, Syracuse, New York 13244-1130 and Materials Science Division, Building 223, Argonne National Laboratory, Argonne, Illinois 60439

P. A. Dowben

Department of Physics, University of Nebraska-Lincoln, Lincoln, Nebraska 68588-0111

(Received 11 October 1993; accepted 28 February 1994)

Using photoelectron spectroscopy, the overlayer electronic structure was observed to be modulated by the Hg growth mode for Hg adsorbed on W(110) at 200 K. The Hg layer-by-layer growth was also characterized by variations in the ratio between the Hg 5*d* shallow core level and W 4*f* photoemission intensities. This layer-by-layer growth occurs in spite of surprisingly weak electronic interactions between the adatoms and the substrate.

I. INTRODUCTION

The overlayer growth modes, surface structures, and electronic properties associated with metal monolayers adsorbed on the different metal surfaces have attracted considerable attention from the surface science community.¹⁻³ Strain and interfacial energies are believed to have a considerable influence on the growth mode.⁴ The influence of the surface structure and anisotropic strain upon growth⁵ is of some significance.

Recently, using photoemission and resonance photoemission, we have observed that the Hg overlayer undergoes a gradual nonmetal to metal transition with increasing Hg coverage on W(110) at 200 K.^{6,7} This gradual transition is due to the gradual increase of the two-dimensional island size and the gradual increase of the average Hg adatom coordination.

The overlayer nonmetal to metal transition corresponds to the changes from localization to delocalization for the overlayer valence electrons. This phase transition relies upon a specific overlayer growth mode, surface structure, surface interaction, and adatom coordination. Essential to the understanding of this phase transition is the characterization of the growth mode. In this paper we demonstrate that the overlayer electronic structure is modulated by the layer-by-layer growth mode on W(110).

II. EXPERIMENTAL DETAILS

The experiments were carried out in an UHV system equipped with a hemispherical analyzer, a retarding-field analyzer for low-energy electron diffraction, described in detail elsewhere.⁸ The light source for the photoemission studies was the 3-m toroidal grating monochromator at the Synchrotron Radiation Center in Stoughton, Wisconsin. The incidence angle of the light is defined with respect to the surface normal. The incident light of 36° or 65° off normal was used to give a larger portion of light with its vector potential parallel to or perpendicular to the surface (*s* or *p* polarization, respectively). The energy analyzer has an acceptance angle of ±1° and the energy resolution of the photoemission spectra, including the light source, varied from

0.12 to 0.2 eV, full width at half-maximum. Relative photoemission intensities were given from the integral counts for a photoemission feature and normalized by the transmitted flux out of the monochromator. The binding energies of the photoemission features are referenced to the Fermi level. The surface work function change was measured by the shift in the secondary photoelectron emission threshold.

The W(110) substrate was cleaned by the accepted procedure of annealing in O₂ and flashing.⁹ Following this procedure, the crystal was cooled to 200 K with the use of a liquid-nitrogen cold stage and the substrate temperature was determined with a W-5%Re/W-26%Re thermocouple. The mercury adsorption was undertaken with techniques described elsewhere.¹⁰ The base pressure was about 7×10⁻¹¹ Torr. The ambient Hg pressure during the adsorption was always less than 2×10⁻⁸ Torr.

III. RESULTS

Figure 1 shows the evolution of the Hg-induced photoemission features and the attenuation of the W(110) photoemission features at normal emission, for different exposures of the W(110) surface at 200 K to Hg vapor. With increasing Hg coverage, the W(110) valence band features become suppressed, while two intense features of the Hg 5*d* spin-orbit doublet at binding energies of 9.8±0.1 eV (5*d*_{3/2}) and 7.8±0.1 eV (5*d*_{5/2}) dominate the spectra. The width of these two features increases gradually with increasing Hg coverage.⁷ A second Hg 5*d*_{5/2} feature at about 7.2±0.1 eV can be seen after about 4 langmuirs (1 langmuir=1 L=10⁻⁶ Torr s) and is increasingly well resolved with increasing coverage. This Hg-induced feature is caused by the hybridization of orbitals between adjacent Hg adatoms.⁷ At smaller binding energies (*E_F* to 7 eV), there are some broad Hg-induced features assigned to the Hg overlayer quantum well states and an interface/surface state.^{7,11}

The adsorption curve was determined by the Hg 5*d* and W 4*f* photoemission signals. The photoemission intensity changes of the Hg 5*d* and the W 4*f* with increasing Hg exposure are shown in Fig. 2(a), and the ratios of intensities

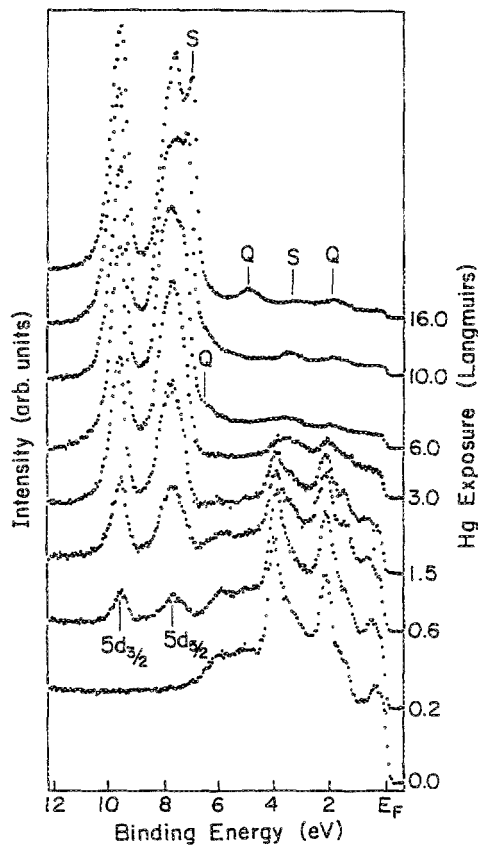


FIG. 1. The photoemission spectra of Hg on W(110) at 200 K with increasing Hg exposure. The photoelectrons were collected normal to the surface. The light incidence angles are 36° . The Hg quantum well states are indicated by Q and the additional Hg overlayer band structure related state and interface/surface state by S. The photon energy is 40 eV.

of the Hg $5d_{3/2}$ and $5d_{5/2}$ to W $4f_{7/2}$ as functions of the Hg exposure are also shown in Fig. 2(b). From the adsorption curve, we suggest that the Hg growth on W(110) at 200 K resembles, very closely, layer-by-layer growth. Previous work by Zhao and Gomer on the same system¹² has also provided evidence for this growth mode. From the adsorption curve (Fig. 2) and the quantum well state intensities (Fig. 3) we estimate that a layer of mercury is established after 4–5 L exposure, and a complete close-packed layer is formed at 8 L. The second layer adsorption results in the “kink” in the adsorption curves (see Fig. 2). The adsorption saturates at a thickness of two monolayers. This result is similar to Hg on Cu(100) where a $c(2 \times 2)$ layer is formed by 5 L and a more close-packed layer is completed by 11 L followed by further adsorption of Hg into a second layer,¹³ although the overlayer structures are different. Hg on Ag(100) also exhibits a similar growth pattern.^{10,14} The difference in exposure necessary for completion of a monolayer on these metal substrates is due to different sticking coefficients and structures.

The slope in the ratio of the Hg $5d$ intensities relative to the intensity of the W $4f$ increases with increasing Hg exposure as shown in Fig. 2(b). These results also suggest that the layer-by-layer growth is dominant in the coverage range up to two monolayers. Any three-dimensional island formation

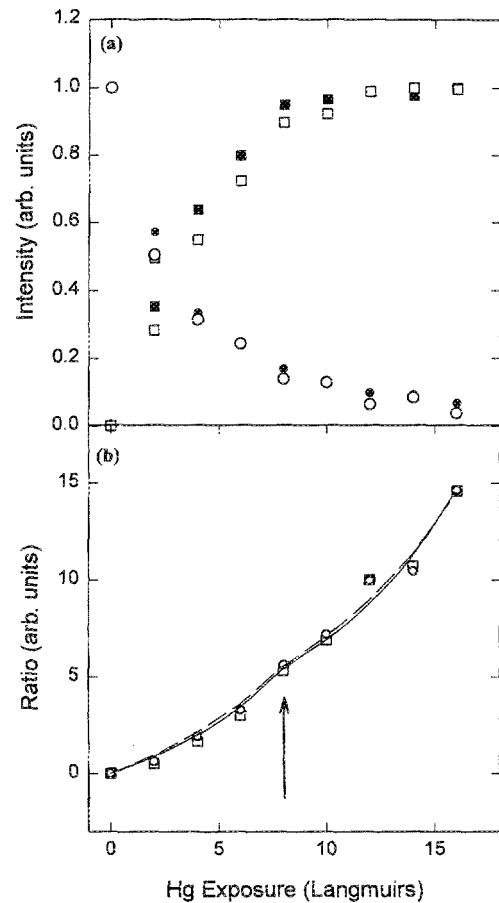


FIG. 2. The Hg adsorption curve on W(110) at 200 K. The photoemission intensity changes of Hg $5d_{3/2}$ (\square) and $5d_{5/2}$ (\blacksquare), W $4f_{5/2}$ (\circ) and $4f_{7/2}$ (\bullet) are shown in (a). The ratios of intensities of Hg $5d_{3/2}$ (\square) and $5d_{5/2}$ (\circ) to W $4f_{7/2}$ are shown in (b). The fitting curves to the ratios of intensities are also shown in (b). Completion of one monolayer is indicated by the arrow.

or amalgamation of the mercury would result in a Hg-to-W signal ratio that changes little with increasing mercury exposure.

If Hg is adsorbed layer by layer, the intensity changes of Hg $5d$ and W $4f$ photoemission with Hg coverage should be given by

$$I^{5d}(\vartheta_n) = I_0^{5d} \left(\frac{1 - e^{-(n-1)\beta_{5d}}}{1 - e^{-\beta_{5d}}} + \vartheta_n e^{-(n-1)\beta_{5d}} \right), \quad (1)$$

$$I^{4f}(\vartheta_n) = I_0^{4f} e^{-(n-1)\beta_{4f}} (1 - \vartheta_n + \vartheta_n e^{-\beta_{4f}}), \quad (2)$$

where the n th layer is being adsorbed on top of $(n-1)$ completed layers ($n \geq 2$). ϑ_n is the coverage in the n th layer, I_0^{5d} the intensity of the Hg $5d$ level and I_0^{4f} the intensity of the W $4f$ level for $n=0$. β (β_{5d} or β_{4f}) is the attenuation parameter which should be dependent on the kinetic energy of electron. The mean free path can be obtained, for either the Hg $5d$ or the W $4f$ electrons, as

$$\lambda_{(5d,4f)} = l / \beta_{(5d,4f)}, \quad (3)$$

where l is the thickness of one Hg monolayer. Then the ratio of the intensities in the n th layer is

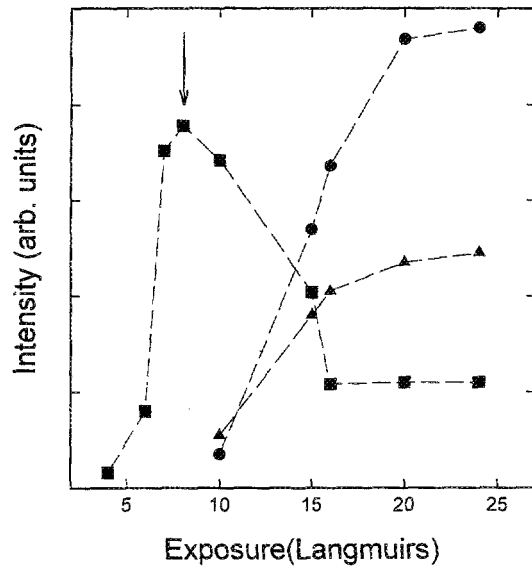


FIG. 3. The intensity changes of the quantum well states with increasing Hg exposure on W(110), (■) the state at 6.6 eV below E_F at $\bar{\Gamma}$, (●) the state at 5.0 eV below E_F at $\bar{\Gamma}$, and (▲) the state at 1.95 eV below E_F at $\bar{\Gamma}$. The photon energy used was 40 eV. The data correspond to the 4° off normal photoemission spectra along $\bar{\Gamma}N$ of the clean W(110) Brillouin zone with p -polarized light. The arrow marks the completion of the first Hg monolayer adsorption on W(110). The dashed curves are just as a guide.

$$\frac{I^{5d}(\vartheta_n)}{I^{4f}(\vartheta_n)} = \frac{I_0^{5d}}{I_0^{4f}} \frac{1 - e^{-(n-1)\beta_{5d}}}{1 - e^{-\beta_{5d}}} + \vartheta_n e^{-(n-1)\beta_{5d}} \quad (4)$$

Since the kinetic energy of outgoing Hg 5d electrons in the photoemission with 40-eV photons is very close to that of outgoing W 4f electrons with 60-eV photons, we can assume that the attenuation parameters are the same, $\beta_{5d} = \beta_{4f}$. Using above result to fit our experimental data [Fig. 2(b)] and taking the diameter of the Hg atom ($\sim 3.0 \text{ \AA}$) as the thickness of one monolayer of Hg, we find that the electron mean free path is about 5.54 \AA for layer by layer growth. If we use the empirical mean-free-path formula¹⁵

$$\lambda = \frac{\epsilon}{a(\ln \epsilon + b)} \quad (5)$$

for electrons with a kinetic energy of 25 eV through a mercury layer ($a=14.5$, $b=-2.7$), then the mean free path is only about 3.32 \AA . The difference between these two results can be caused by the fact that the simple empirical theory is not strictly valid for such low kinetic energy electrons.

Further evidence for layer-by-layer growth can be observed in the intensity variations of the Hg overlayer quantum well states (Fig. 3). The state at 6.6 eV below E_F (at $\bar{\Gamma}$) identified as the quantum well state of a monolayer⁷ reaches a maximum at 8 L exposure. The states attributable to the mercury bilayer, at 5.0 and 1.95 eV,⁷ appear only at 10 L exposure. The bilayer quantum well state intensities increase as the monolayer quantum well intensity declines (Fig. 3).

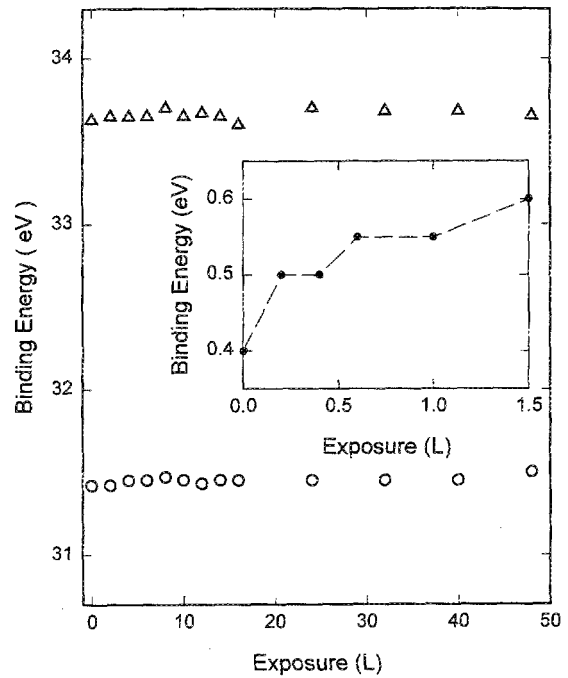


FIG. 4. The W 4f binding energy changes vs Hg exposure. The data were taken at normal emission using 60-eV p -polarized light. The binding energy change of the W(110) surface state just below E_F as function of Hg exposure is shown in the inset (photon energy was 40 eV).

These results are also consistent with the results obtained using mean-free-path arguments that the Hg overlayer saturates at two monolayers.

The development of W 4f ($4f_{5/2}$ and $4f_{7/2}$) and W(110) surface state binding energies with increasing Hg coverage are shown in Fig. 4. As seen in Fig. 1, while the W(110) photoemission features are largely attenuated for Hg coverage beyond half monolayers (4 L), their binding energies are largely unaffected by the Hg overlayer. The W(110) 2.05- and 4.05-eV valence band features do not alter in binding energy with Hg adsorption. Only the surface state (see the inset to Fig. 4) is seen to be slightly affected by the Hg adsorption. With increasing Hg coverage, the W(110) surface state just below the Fermi energy shifts to higher binding energy from 0.4 eV for the clean surface (as seen from Fig. 4) and attenuates evenly. This state is one of W 5d surface states with d_{z^2} character.¹⁶

The binding energies (determined from the vertical peak position) of the all Hg-induced features as a function of the Hg coverage are shown in Fig. 5. The Hg second $5d_{5/2}$ induced state at about 7.2 eV of $d_{xz,yz}$ character⁷ changes its binding energies with Hg coverage periodically as shown in Fig. 6. This periodic behavior attenuates with increasing coverage (or the number of monolayers in the Hg adsorption). The features reach minima in the binding energy at the completion of a monolayer and a bilayer (at 8 and 16 L).

The work function change exhibits typical features of a metal overlayer adsorbed on a metal surface¹⁷ and is similar to the results obtained by Zhao and Gomer,¹² except for the great differences in coverage calibration. Initially the work function decreases almost linearly from 5.06 eV [which is

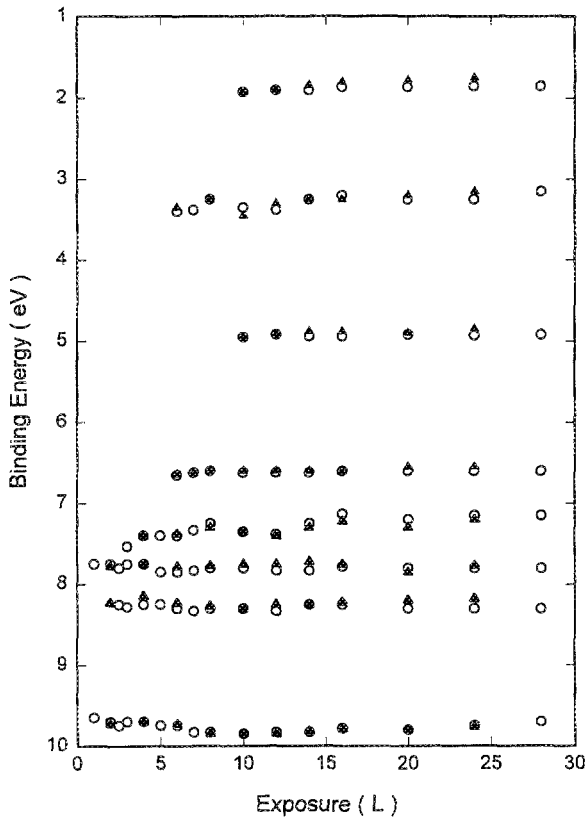


FIG. 5. The coverage-dependent binding energies of all overlayer photoemission features with both *s*-polarized light (○) and *p*-polarized light (▲). The photon energy was 40 eV.

close to the intrinsic work function on the W(110) surface] and then the curve flattens and reaches a shallow minimum ($\phi_{\min}=4.4$ eV, $\Delta\phi_m=-0.66$ eV) at about 9 L (ϑ_m), consistent with our assignment of a monolayer (8 L). At about two

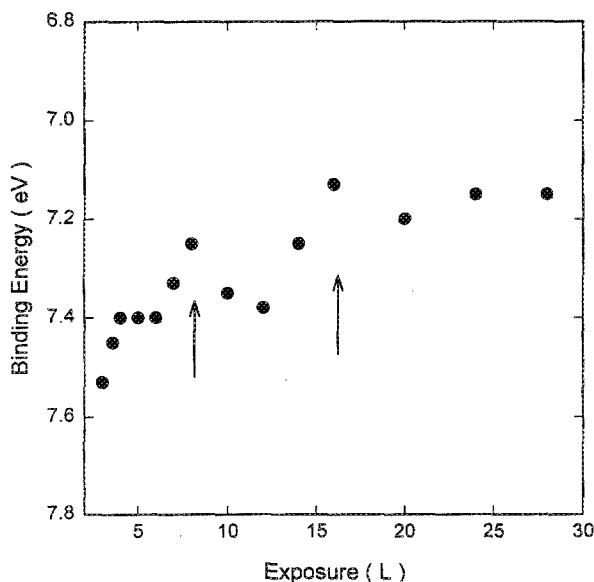


FIG. 6. The binding energies of the Hg second $5d_{5/2}$ feature vs Hg exposure, with *s*-polarized light. Completion of Hg monolayers 1 and 2 is indicated by the arrows. The photon energy was 40 eV.

monolayers (or 16 L), the work function of bulk mercury is approached.

IV. DISCUSSION

For at least two monolayers, Hg adsorption on W(110) is layer-by-layer growth. This is clear from several different techniques: work function, quantum well state intensities, Hg $5d_{xz,yz}$ binding energy shifts, and the substrate signal attenuation. All our evidence suggests weak bonding of the Hg adlayer in spite of the layer-by-layer growth.

According to the classical-phenomenological description for the work function change with change of adsorbate coverage,^{17,18} the linear decrease of the work function is due to the charge transfer between adatoms and substrate and the formation of surface dipole moments at initial coverage. With increasing coverage, a departure from the linear dependence of $\Delta\phi$ on coverage is attributed to a dipole depolarization. This progressive neutralization decreases in turn the dipole moment per atom, normally leading to a minimum in work function versus coverage curve. At the saturation coverage, which is generally close to the atomic density of a close-packed layer of adatoms, the work function approaches the work function of adsorbate material in the bulk.

For our system, we can exclude the completely ionized model on the basis of the empirical relation¹⁹

$$\Delta\phi_m = 1.24 \left(\phi_0 - \frac{I_A + E_A}{2} \right), \quad (6)$$

where ϕ_0 (5.06 eV) is the intrinsic work function of the clean surface, I_A the first ionization potential, and E_A the electron affinity of the adsorbate. This implies that $\Delta\phi_m = -1.04$ eV from the above equation, quite different from our measured value of $\Delta\phi_m = -0.66$ eV,⁷ though we cannot exclude the effects of initial stages of growth and the structural changes that the overlayer may adopt. These structural changes may result in complicated (though small) changes in Hg binding energies as well (Fig. 6).

A more accurate picture of the work function change during the adsorption process and the formation of the dipole moment can be best described here as a result of polarization of the adsorbate^{20,21} rather than electron transfer. This adatom polarization is attributable to the hybridization of electron wave functions between adatom and substrate. The coverage corresponding to the work function minimum occurs when the surface bonding changes from "covalent" to "metallic." In addition to the temperature and lateral interaction effects, the depth of the work function minimum and the position of the minimum (ϑ_m) are dependent on the adatom polarization effect (initial surface bonding). The weak surface bonding will cause only a shallow minimum in the work function change consistent with results obtained for Hg on W(110). Furthermore, from the initial work function change we find that the initial dipole moment μ_0 ($\mu_0 \sim d\phi/d\theta$ when $\vartheta \rightarrow 0$) is only $0.044 e \text{ \AA}$. The charge transfer between the adatoms and the substrate should, therefore, be very small, at best.

The weak surface covalent bonding is also indicated by the evolution of the surface electronic structure of the Hg

overlayer on W(110). The insignificant W 4*f* binding energy shift of less than 0.1 eV also indicates that there is little charge transfer between the Hg adatoms and the substrate and/or little influence on the final state binding energy. As seen from Fig. 5, the overlayer core levels—Hg 5*d*_{3/2} and Hg 5*d*_{5/2}—also shift only 0.1 eV (or less) with increasing Hg concentration. This small binding energy shift, combined with the small shift of W 4*f* core levels, support the weak bonding model of the Hg adsorption. Recent work in understanding Hg on Ni(111) notes that there is little contribution of the Hg 5*d* electrons to the substrate bonding.²²

The adsorbate-induced binding energy shifts of W(110) surface states with adsorption of an adlayer have been observed in many other systems, like Hg/W(100),²³ Cs/W(100),²⁴ Cs/Ta(100),²⁴ Cs/Mo(100),²⁴ and Cs/Cu(111).²⁵ According to Wimmer *et al.*²⁰ and Soukiassian *et al.*,²⁴ the electronic origin of the surface state shifts can be understood to be the result of the formation of bonds between the *d*-like surface state of substrate and the *s*-derived valence states of adsorbate. When the adatoms are adsorbed on the surface, the surface state forms bonds with the adatom *s*-derived state. As a result, the binding energy of the hybridized bonding state is higher than that of the surface state on a clean surface. The magnitude of the binding energy change should be roughly proportional to the strength of the surface bonding. Comparing the shift of the W surface states with alkali or other metal deposition,²⁴ the small shift [only about 0.2 eV compared with the 1.0-eV shift observed for the W *d*_{z²} surface state in the Cs/W(100) system] of the surface state by Hg adsorption is consistent with our postulate that the adlayer bonds weakly with the substrate. The core level binding energies and work function indicate little charge transfer, and, as noted above, Hg desorbs from W(110) below room temperature. We conclude that there is little hybridization of the Hg overlayer electronic states with the W(110) states.

For the adsorption on W(110) at room temperature, there are no Hg-induced features appearing in the photoemission spectra even for 15–20 L Hg exposure. This again suggests that the bonding between the Hg atoms and the substrate is quite weak, even weaker than is observed for the Hg on W(100),²³ where adsorption at room temperature is observed.

Layer-by-layer growth has an interesting influence on the development of the overlayer electronic structure. As we reported previously,^{6,7,13,26} The second Hg 5*d*_{5/2} feature at 7.2 ± 0.1 eV is due to orbital hybridization between the adjacent adatoms, largely of *d*_{xz} and *d*_{yz} character, and is characteristic of the Hg overlayer. The periodic change in binding energy with Hg coverage corresponds to the completion of each monolayer (as seen from Fig. 6). This reflects the periodic change of the average adatom coordination because of the relative change of island edge sites due to layer-by-layer growth.^{6,7,27} This effect of coordination on binding energy has been observed for other overlayers.^{27,28}

V. SUMMARY

Layer-by-layer growth of Hg adsorption on W(110) at 200 K was probed by photoemission. The change of surface work function and valence electronic structure of both the W sub-

strate and Hg overlayer suggests that the surface bonding is weak but adatom–adatom bonding (coordination) does affect the binding energies of the Hg-induced features.

The periodic binding energy change of the second Hg 5*d*_{5/2} feature, which reflects the coordination of the Hg adatoms, is influenced by the overlayer layer-by-layer growth. This effect is expected.²⁷

ACKNOWLEDGMENTS

The authors would like to thank Dr. M. Onellion and Dr. E. W. Plummer for a number of helpful discussions. This work was supported by the National Science Foundation (NSF) through Grant No. DMR-92-21655 and was undertaken at the Synchrotron Radiation Center in Stoughton, Wisconsin, which is supported by the NSF.

¹E. Bauer, *The Chemical Physics of Solid Surfaces and Heterogeneous Catalysis*, edited by D. A. King and D. D. Woodruff (Elsevier, New York, 1984), Vol. 3.

²A. Chamberod and J. Hillairet, *Metallic Multilayers*, Materials Science Forum (1990), Vols. 59 and 60.

³P. A. Dowben, M. Onellion, and Y. J. Kime, *Scan. Microsc.* **1**, 177 (1988).

⁴J. H. van der Merwe, *J. Appl. Phys.* **41**, 4725 (1970); *Treatise on Material Science and Technology*, edited by H. Herman (Academic, New York, 1973) Vol. 2, p. 90; I. Markov and S. Stoyanov, *Comtemp. Phys.* **28**, 267 (1987).

⁵M. Vos and I. V. Mitchell, *Phys. Rev. B* **45**, 9398 (1992).

⁶J. Zhang, D. Li, and P. A. Dowben, *Phys. Lett. A* **173**, 183 (1993).

⁷J. Zhang, D. Li, and P. A. Dowben, *J. Phys. Condes. Matt.* **6**, 33 (1994).

⁸P. A. Dowben, D. Lagraffe, and M. Onellion, *J. Phys. Condes. Matter* **1**, 6571 (1989).

⁹A. Horlacher-Smith, R. A. Barker, and P. J. Estrup, *Surf. Sci.* **136**, 329 (1984); L. D. Roelofs, J. W. Chung, S. C. Ying, and P. J. Estrup, *Phys. Rev. B* **33**, 6537 (1986).

¹⁰P. A. Dowben, Y. J. Kime, S. Varma, M. Onellion, and J. L. Erskine, *Phys. Rev. B* **36**, 2519 (1987).

¹¹D. Li, J. Zhang, and P. A. Dowben (unpublished).

¹²Y. B. Zhao and R. Gomer, *Surf. Sci.* **271**, 85 (1992).

¹³P. A. Dowben, D. LaGraffe, Dongqi Li, G. Vidali, L. Zhang, L. Dotti, and M. Onellion, *Phys. Rev. B* **43**, 10 677 (1991).

¹⁴M. Onellion, J. L. Erskine, Y. J. Kime, S. Varma, and P. A. Dowben, *Phys. Rev. B* **33**, 8833 (1986).

¹⁵C. J. Powell, *Surf. Sci.* **44**, 29 (1974); D. R. Penn, *J. Electron. Spectrosc. Relat. Phenom.* **9**, 29 (1976); M. P. Seah and W. A. Dench, *Surf. Interface Anal.* **1**, 2 (1979).

¹⁶M. W. Holmers, D. A. King, and J. E. Inglesfield, *Phys. Rev. Lett.* **42**, 394 (1979); R. H. Gaylord and S. D. Kevan, *Phys. Rev. B* **36**, 9337 (1987); R. H. Gaylord, K. H. Jeong, and S. D. Kevan, *Phys. Rev. Lett.* **64**, 2036 (1989).

¹⁷J. Hölzl and F. K. Schulte, in *Springer Tracts in Modern Physics*, edited by G. Hohler and E. A. Niechich (Springer, Berlin, 1979), Vol. 85.

¹⁸J. Hölzl and L. Fritsche, *Surf. Sci.* **247**, 226 (1991); I. Langmuir, *J. Am. Chem. Soc.* **54**, 2798 (1932); D. M. Newns, *Phys. Rev. Lett. A* **33**, 43 (1970); P. W. Anderson, *Phys. Rev.* **124**, 41 (1961).

¹⁹G. O. Alton, *Surf. Sci.* **175**, 226 (1986).

²⁰E. Wimmer, A. J. Freeman, M. Weinert, H. Krakauer, J. R. Hiskes, and A. M. Karo, *Phys. Rev. Lett.* **48**, 1128 (1982); E. Wimmer, A. J. Freeman, J. R. Hiskes, and A. M. Karo, *Phys. Rev. B* **28**, 3074 (1983); H. Ishida and K. Terakura, *ibid.* **38**, 5752 (1988); **36**, 4510 (1986); H. Ishida, *ibid.* **38**, 8006 (1988); **39**, 5492 (1989).

²¹B. Woratschek, W. Sesselmann, J. Kupperts, and G. Ertl, *Phys. Rev. Lett.* **55**, 1231 (1985); D. M. Riffe, G. K. Weithelm, and P. H. Citrin, *ibid.* **64**, 571 (1990); X. Shi, D. Tang, D. Heskett, K.-D. Tsuei, H. Ishida, Y. Morikawa, and K. Terakura, *Phys. Rev. B* **47**, 4014 (1993); X. Shi, D. Tang, D. Heskett, K.-D. Tsuei, H. Ishida, and Y. Morikawa, *Surf. Sci.* **290**, 69 (1993); L. A. Hemstreet and S. R. Chubb, *Phys. Rev. B* **47**, 10 748 (1993).

- ²²N. K. Singh, D. Dale, D. Bullett, and R. G. Jones, *Surf. Sci.* **294**, 333 (1993).
- ²³W. F. Egelhoff, Jr., D. L. Perry, and J. W. Linnett, *Surf. Sci.* **54**, 670 (1976).
- ²⁴P. Soukiassian, R. Riwan, J. Lecante, E. Wimmer, S. R. Chubb, and A. J. Freeman, *Phys. Rev. B* **31**, 4911 (1985); P. Soukiassian, R. Riwan, and Y. Borensztein, *Solid State Commun.* **44**, 1375 (1979).
- ²⁵S. A. Lindgren and L. Wallden, *Chem. Phys. Lett.* **64**, 239 (1979).
- ²⁶Dongqi Li, Jiandi Zhang, Sunwoo Lee, and P. A. Dowben, *Phys. Rev. B* **45**, 11 876 (1992).
- ²⁷M. Salmeron, S. Ferrer, M. Jazzar, and G. A. Somorjai, *Phys. Rev. B* **28**, 1158, 6758 (1983).
- ²⁸D. LaGraffe, P. A. Dowben, and M. Ocellion, *Phys. Rev. B* **40**, 3348 (1989).